Article

pubs.acs.org/Biomac

Enzyme Responsive Hyaluronic Acid Nanocapsules Containing Polyhexanide and Their Exposure to Bacteria To Prevent Infection

Grit Baier,[†] Alex Cavallaro,[‡] Krasimir Vasilev,[‡] Volker Mailänder,[†,§] Anna Musyanovych,[†] and Katharina Landfester*[,†]

[†]Max Planck Institute for Polymer Research, Ackermannweg 10, 55128 Mainz, Germany

[‡]Mawson Institute, University of South Australia, Mawson Lakes SA 5095, Australia

[§]IIIrd Medical Clinic, Hematology, Oncology and Pulmonology, University Medicine of the Johannes Gutenberg University, Mainz, Langenbeckstrasse 1, 55131 Mainz, Germany

Supporting Information

ABSTRACT: Antibacterial nanodevices could bring coatings of plastic materials and wound dressings a big step forward if the release of the antibacterial agents could be triggered by the presence of the bacteria themselves. Here, we show that novel hyaluronic acid (HA)-based nanocapsules containing the antimicrobial agent polyhexanide are specifically cleaved in the presence of hyaluronidase, a factor of pathogenicity and invasion for bacteria like *Staphylococcus aureus* and *Escherichia coli*. This resulted in an efficient killing of the pathogenic bacteria by the antimicrobial agent. The formation of different polymeric nanocapsules was achieved through a polyaddition reaction in inverse miniemulsion. After the synthesis, the nanocapsules were transferred to an aqueous medium and investigated in terms of size, size distribution, functionality, and morphology using dynamic light scattering, zeta potential measurements and scanning electron microscopy. The enzyme triggered release of a model dye and the antimicrobial polyhexanide was monitored using fluorescence and UV spectroscopy. The stability of the nanocapsules in several biological media was tested and the interaction of nanocapsules with human serum protein was studied using isothermal titration calorimetry. The antibacterial effectiveness is demonstrated by determination of the antibacterial activity and determination of the minimal bactericidal concentration (MBC).

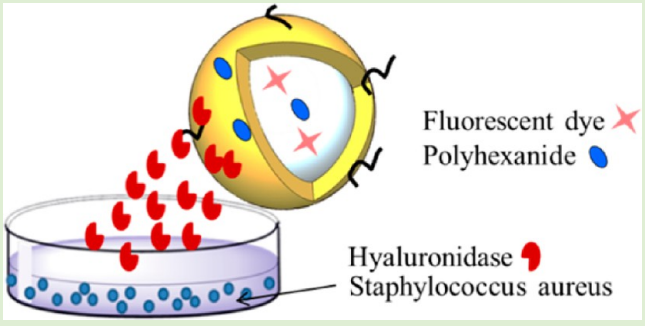

INTRODUCTION

Wounds and indwelling catheters literally open up huge opportunities for the invasion and proliferation of pathogenic bacteria and thus cause bacterial infection. After initial, superficial adhesion of bacteria to wounds and plastic materials, further spreading requires the use of enzymes as invasion factors.[1] They have been detected as secreted factors that enable the penetration of deeper tissues. These invasion factors are important pathogenicity. One of the first invasion factors for tissues discovered was hyaluronidase, an enzyme that degrades hyaluronic acid (also known as hyaluronan) or its salt, the hyaluronate.[2,3] By degrading, part of the extracellular matrix infiltration is drastically enhanced. The enzyme hyaluronidase, which is capable to degrade hyaluronic acid, is produced by a wide variety of pathogenic Gram-positive bacteria (e.g., streptococcus). Among the staphylococci, hyaluronidase production has been shown for pathogenic strains of *Staphylococcus aureus*.[4] The hyaluronidase activity of a selected group of staphylococcal species was published by Hart et al.[5] Saltos et al. reviewed the array of reactions (enzymatic, free radical and chemical based reactions) which cause the cleavage of hyaluronic acid.[6] Interestingly, hyaluronic acid (HA) also shows bacteriostatic effects[7] and recent investigations suggest antimicrobial and antiviral properties for HA, as it was studied for clinically relevant bacterial and fungal species.[8]

The bacterial contamination of wounds like burns is a problem that is not yet under complete control. In the case of an invasive wound infection, there is a high risk that will progress to a general sepsis. This is mainly due to the presence of *S. aureus* bacteria, which are able to penetrate and to infiltrate subcutaneous tissues followed by hematogenous spreading. Wound care is therefore focused on infection prevention with the need for smart and responsive materials. We want to point out that first besides the hyaluronidase from bacteria also hyaluronidase from mammalian cells can be found in tissues as also in wounds.[9] Furthermore, hyaluronic acid nanocapsules could bind to the CD44 receptor on leukocytes hereby triggering the undesired uptake of free nanocapsules.[10] For application of these nanocapsules, this needs to be circum-

Received: December 30, 2012
Revised: February 28, 2013
Published: February 28, 2013

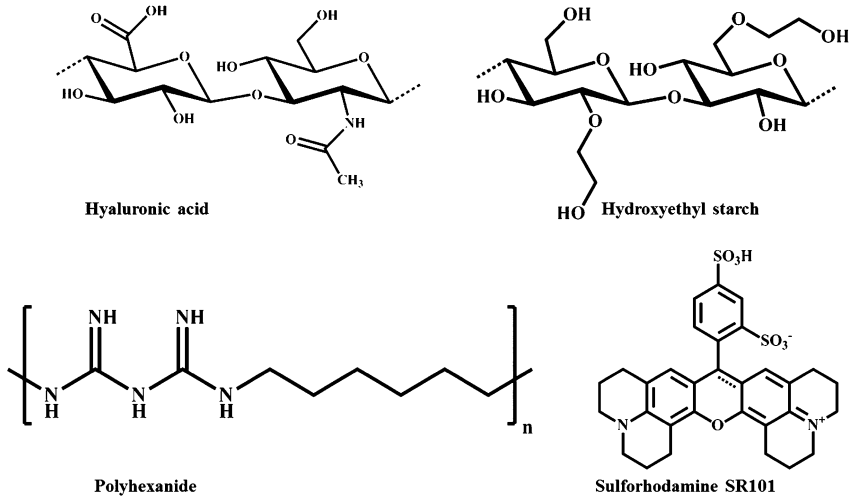

Figure 1. Chemical structures of hyaluronic acid, hydroxyethyl starch, polyhexanide and the dye sulforhodamine SR101.

vented by immobilizing the nanocapsules tightly enough on a substrate like a wound dressing.

Furthermore, hyaluronic acid is also important in wound healing processes. It is known to promote early inflammation which is critical for initiating wound healing, while at later times, it contributes to matrix stabilization, thus participating down regulation of inflammatory reactions.[11−13] Because of its biological properties, including nonimmunogenicity which is an essential prerequisite for biocompatibility,[14] this anionic glycosaminoglycan consisting of glucuronic acid and *N*-acetyl glucosamine disaccharide units has several clinical applications.

In case of burn wounds, the immunological competence is severely impaired, and therefore, the local antiseptic wound treatment is an essential goal in the therapy of burn injuries. The antimicrobial properties of different antiseptic agents have been presented in several studies. In the publication of Koburger et al.,[15] a comparative investigation of antimicrobial efficacy of the antiseptics like triclosan, PVP-iodine, octenidine dihydrochloride, polyhexidine, and chlorhexidine has been shown. Using a prolonged contact time, polyhexanide and octenidine were found to be highly recommended, whereby polyhexanide seems to be preferable for wounds due to its high tolerability.[16] Another group studied the minimum inhibitory (MIC) and minimum microbicidal concentration (MMC) of polyhexanide against antibiotic sensitive and resistant *S. aureus* and *Escherichia coli* strains.[17] In another study, both antimicrobials (polyhexanide and octenidine) were found as the most suitable agents with a high biocompatibility index and very suitable for use in clinical practice.[18] Especially, the cationic poly(hexamethylene biguanide) hydrochloride (PHMB, polyhexanide) is a most widely used antiseptic, due to its excellent antimicrobial activity, chemical stability, low toxicity, and reasonable cost.[19] Furthermore, it is shown that polyhexanide in low concentrations stimulates the cell proliferation and promotes wound healing in animal models.[20,21]

The miniemulsion process offers the ability to produce polymeric nanocapsules in a size range between 100 and 500 nm with controlled properties, that is, average size, morphology, and surface functionality. Under carefully chosen conditions of miniemulsification, it is possible to encapsulate efficiently fragile molecules like DNA, peptides, and so forth.[22,23] The high stability of the system allows performing the reactions inside the droplets and at their interface.[24]

The goal for this paper was to utilize the secretion of hyaluronidase by Gram-positive staphylococcus bacteria (*S. aureus*) leading to the desired cleavage of hyaluronic acid (HA)-based nanocapsules followed by the release of polyhexanide (PH). Biocompatible polymeric HA-based nanocapsules were synthesized by interfacial polyaddition reaction performed in an inverse (water-in-oil) miniemulsion system. PH was encapsulated inside the nanocapsules, which counteracts the pathogenic bacteria in wounds. The hyaluronidase triggered release of PH and the cleavage of the HA-based nanocapsules were investigated by measuring the absorbance. In addition, the interaction of different nanocapsules with proteins from the human serum was studied by isothermal titration calorimetry (ITC) which is an important tool to determine the interaction with the prevailing proteins whenever nanocapsules get in contact with the wound environment.

MATERIALS AND METHODS

Chemical Reagents. All chemicals or materials were used without further purification. Demineralized water was used during the experiments. Hyaluronic acid sodium salt (M_w =140 000 g·mol^{-1}) was purchased from Fluka. The magnesium- and calcium-free phosphate buffered solution (PBS buffer) was purchased from Gibco, Germany. The antimicrobial agent polyhexanide (polyhexamethylene biguanide, PHMB, M_w = 2000 g·mol^{-1}) was purchased from Fagron, Germany. Hydroxyethyl starch (HES, 10%, degree of molar substitution = 0.5, M_w = 200 000 g·mol^{-1}) was purchased from Fresenius Kabi, Germany. The hyaluronidase from bovine tests was purchased from Sigma Aldrich. The phosphate buffer (0.02 M, pH 7, with 77 mM sodium chloride (Sigma) and 0.01% BSA (Fluka)) was freshly prepared from potassium dihydrogen phosphate (Sigma) and from the sodium salt of phosphoric acid (Sigma). 2,4-Toluene diisocyanate (TDI) and cyclohexane (>99.9%) were purchased from Sigma Aldrich. The oil soluble block copolymer surfactant poly-[(ethylene-*co*-butylene)-*b*-(ethylene oxide)], P(E/B-*b*-EO), consisting of a poly(ethylene-*co*-butylene) block (M_w = 3700 g·mol^{-1}) and a poly(ethylene oxide) block (M_w = 3600 g·mol^{-1}), was synthesized according to the procedure described in the literature.[25] The nonionic surfactant Lutensol AT50, which is a poly(ethylene oxide)-hexadecyl ether with an ethylene oxide (EO) block length of about 50 units, was provided from BASF, Germany. The fluorescent dye sulforhodamine 101 (SR101) was purchased from BioChemica. The sodium chloride (NaCl 0.9%) and the Ringer solution were purchased from Fresenius Kabi. The magnesium- and calcium-free phosphate buffered solution

(PBS) was purchased from Invitrogen. The human serum was pooled from 10 donators according to the approval of the local ethics committee and kindly collected by Transfusion Center Mainz. The CASO broth for the bacterial tests was purchased from Roth. The chemical structures of hyaluronic acid, hydroxyethyl starch, polyhexanide and sulforhodamine SR 101 are depicted in Figure 1.

Preparation of the Nanocapsules. Hyaluronic acid nanocapsules (HA-NCs) and hydroxyethyl starch nanocapsules (HES-NCs) (with and without the antimicrobial agent polyhexanide) were synthesized via interfacial polyaddition reaction using the inverse miniemulsion technique according to the procedure described previously[26,27] with slight changes as described in this section. Briefly, an aqueous phase consisting of the ingredients, see Table 1, was mixed with PBS buffer. In the case of HA, the samples were treated in an ultrasonication bath and stirred overnight to be sure that all of the hyaluronic acid was dissolved (solution I). The obtained solution was mixed with 1 mg of sulforhodamine SR101 solution (2 mM). The amphiphilic block copolymer poly(ethylene/butylene-*block*-ethylene oxide) P(E/B-*b*-EO) (100 mg) was dissolved in 7.5 g of cyclohexane and mixed with the previously prepared solution I. The obtained emulsion was stirred over 1 h at 25 °C and then ultrasonicated for 180 s at 90% amplitude in a pulse regime (20 s sonication, 10 s pause) using a Branson Sonifier W-450-Digital and a 1/2″ tip under ice cooling. A solution consisting of 5.0 g of cyclohexane, 30 mg of P(E/B-*b*-EO) and 100 mg of TDI was added dropwise over 5 min to the earlier prepared emulsion maintaining the temperature at 25 °C. The reaction proceeded for 24 h at 25 °C under stirring. After the synthesis, nanocapsules were purified by repetitive centrifugation (Sigma 3k-30, RCF 3300, 20 min, two times) in order to remove the residues of surfactant and the pellet was redispersed in cyclohexane. Afterward, the nanocapsules were transferred into an aqueous phase using the following procedure: 1 g (polymer solid content around 3%) of the nanocapsule dispersion in cyclohexane was mixed with 5 g of Lutensol AT50 aqueous solution (0.1 wt %) under mechanical stirring for 24 h at 25 °C. Then, the samples were redispersed for 20 min in a sonication bath (power 50%, 25 kHz). After redispersion, the nanocapsules were cleaned by repetitive centrifugation (Sigma 3k-30, RCF 1467, 20 min, 3 times) in order to remove the residues of the surfactant Lutensol AT50.

Table 1. Composition of the Dispersed Aqueous Phase for the Capsule Formation

samples	amount of			
	HES	HA (mg)	PH (mg)	PBS buffer (μL)
HA-NCs	-	20	-	1380
HA-PH-NCs	-	20	21	1359
PH-NCs	-	-	50	1350
HES-NCs	100	-	-	1300
HES-PH-NCs	79	-	21	1300

Characterization of the Nanocapsules. The average size and the size distribution of the nanocapsules were measured by means of dynamic light scattering (DLS) with diluted dispersions (40 μL of sample was diluted in 1 mL of water) on a PSS Nicomp Particle Sizer 380 (Nicomp Particle Sizing Systems) equipped with a detector at 90° scattering mode at 20 °C. The zeta potential of the nanocapsules was measured in 10^{-3} M potassium chloride solution with a Zeta Nanosizer (Malvern Instruments, U.K.) at 20 °C. Scanning electron microscopy (SEM) studies were done on a field emission microscope (LEO (Zeiss) 1530 Gemini, Oberkochen, Germany) working at an accelerating voltage of 170 V. Generally, the samples were prepared by diluting the capsule dispersion in cyclohexane or demineralized water (for redispersed samples) to about 0.01% solid content. Then one droplet of the sample was placed onto silica wafer and dried under ambient conditions overnight. No additional contrast agent was applied. The solid content of the capsule dispersion was measured gravimetrically. The analysis of the polymer was performed by FTIR measurements. The sample powder was obtained by freeze-drying of the capsule dispersion for 48 h at −60 °C under reduced pressure. Three milligrams of the dry sample was pressed with KBr to form a pellet and a spectrum between 4000 and 400 cm^{-1} was recorded using the IFS 113v Bruker spectrometer. The fluorescence intensities and the absorption values for all mentioned experiments were measured using a plate reader (Infinite M1000, Tecan, Switzerland).

Release Experiments. *Release of Encapsulated Fluorescent Dye out of NCs.* For the release experiments, a phosphate buffer (0.02 M, pH 7, with 77 mM sodium chloride and 0.01% BSA) was freshly prepared 30 min before use. The enzyme hyaluronidase was dissolved, yielding a clear solution. The pH of the nanocapsules was adjusted to pH 5.0, which is the optimum pH for the hyaluronidase activity.[28,29] After addition of the hyaluronidase to nanocapsules (studied concentrations: 32, 16, 8, and 1 mg·mL^{-1}), the samples were gently shaken at 37 °C and the kinetic of fluorescent dye release upon degradation of nanocapsules was studied up to 24 h. After given periods of time, nanocapsules were sedimented by centrifugation (Sigma 3k-30, RCF 1467, 20 min) and the fluorescence of supernatant was measured by a fluorescence spectrometer (microplate reader, Infinite M1000, Tecan, Switzerland). The fluorescent dye SR101 absorbs light at 580 nm and emits light at 605 nm. The total release of SR101 out of the nanocapsules was calculated as a difference between the fluorescent intensities of the supernatant obtained from the samples with and without hyaluronidase treatment. For the data normalization, a total amount of 1×10^{13} NCs/mL (solid content 8 mg/mL) was used for each experiment. The fluorescence signal was normalized to nanocapsules per milliliter at each point of measurement. For each sample, the release of fluorescent dye was calculated from six single measurements and the entire experiment was repeated three times.

Release of Encapsulated Polyhexanide and Cleavage of NCs. For the release of PH from the nanocapsules, the same enzyme treatment procedure as described above was used. After given time periods (0, 1, 2, 4, 7, and 23 h), nanocapsules were sedimented by centrifugation (Sigma 3k-30, RCF 1467, 20 min) and the absorption was measured at 236 nm in the supernatant. The total release of PH from the nanocapsules was calculated as a difference between the absorbance intensities of the supernatant obtained from the samples with and without hyaluronidase treatment. For the data normalization, a total amount of 1×10^{13} NCs/mL (solid content 8 mg/mL) was used for each experiment. For each sample, the release of polyhexanide was calculated from four single measurements and the entire experiment was repeated two times. For the cleavage experiments, the absorption of the nanocapsules dispersion at 231 nm was measured. Experimental setup, data normalization and repetition rate are the same as described above.

Monitoring of the Enzyme Triggered Degradation Process Using DLS and SEM. The average size and the size distribution of the nanocapsules before and after enzyme treatment were measured by means of dynamic light scattering (DLS) and scanning electron microscopy (SEM) using always the same conditions described in the characterization part above. Therefore, the different nanocapsules were treated as described in the part Release Experiments, see above. After the enzyme exposure, the nanocapsules were purified by repetitive centrifugation (Sigma 3k-30, RCF 3300, 20 min) in order to remove the residues of the hyaluronidase, and were subjected to DLS and morphology studies.

Determination of Antibacterial Activity *in Vitro*. The nanocapsules were assayed for activity against *S. aureus* (ATCC 29213 and ATCC 43300) and *E. coli* (ATCC 25922) *in vitro*. Bacteria were plated on Luria−Bertani Agar plates from frozen stocks and incubated at 37 °C. Individual bacterial colonies were picked and incubated overnight at 37 °C in Tryptic Soy Broth (TSB). The nanocapsules were washed and serially diluted in quadruplicate in a 96 well microtiter plate with a final volume of 40 μL per well. ABS_{600} was used to adjust to approximately 1×10^8 CFU·mL^{-1} and further diluted to 1.25×10^6 CFU·mL^{-1} in TSB. A total of 160 μL of bacterial suspension was added to each well to achieve a final concentration of approximately 1

$\times 10^6$ CFU·mL^{-1}. The final concentrations of nanocapsules in the wells ranged from 1000 to 1.9 μg·mL^{-1}. Bacterial suspensions without nanoparticles and wells containing particles and TSB without bacteria were used as controls. Using a microtiter plate reader (Biotek, ELx800), the minimal inhibitory concentration (MIC, the lowest concentration of an antimicrobial that will inhibit the visible growth of a microorganism after overnight incubation) values were determined by measuring the turbidity of the bacterial suspension after 24 h incubation at 37 °C. The effect of light scattering induced by the nanocapsules was taken into account when reading ABS_{600}. The results were confirmed visually. The minimum bactericidal concentration (MBC, the lowest concentration of antibiotic required to kill a particular bacterium) was determined by subculture of a sample from the wells, post MIC study, on Luria–Bertani agar plates. The lowest concentration showing no apparent bacterial growth on a sterile LB-agar plate was determined to be the MIC. All assays were performed in triplicate.

Stability of Nanocapsules in Biological Media. The colloidal and chemical stability of nanocapsules was studied in sodium chloride (NaCl) 0.9%, Ringer's solution, DPBS buffer, human serum and with CASO broth. One milliliter of the NC dispersion was centrifuged, the supernatant was removed and the pellet was redispersed either in NaCl 0.9%, in Ringer's solution, or in DPBS buffer. In the case of human serum and CASO broth, 1 mL of nanocapsules dispersion was mixed with 1 mL of human serum (69 mg protein/mL) or CASO broth. All obtained dispersions were investigated in terms of size and size distribution using DLS. The release of SR101 from the nanocapsules was studied by fluorescence spectroscopy in supernatant: 500 μL of nanocapsules (1×10^{13} nanocapsules/mL, solid content 1%) were mixed with 500 μL of NaCl 0.9% (or Ringer's solution, or DPBS, human serum, or CASO broth), incubated at 37 °C for 24 h and then centrifuged (Sigma 3k-30, RCF 1467, 20 min).

Isothermal Titration Experiments (ITC). The calorimetric measurements were performed using the isothermal titration calorimeter CSC 4200 (Calorimetry Science Corporation). The polymeric nanocapsules were used at a concentration of 10 g·L^{-1} (1×10^{13} nanocapsules/mL) and human serum at a protein concentration of 69 g·L^{-1}. The reaction was started by human serum titration, and in the end, a total volume of 250 μL (50×5 μL) was titrated. The time between the titration steps was 300 s and was chosen to reach an equilibrium state. During all experiments, the temperature of the ITC device was kept constant at 25 °C. The volume of the sample and reference cell was 1.3 mL. The reference cell was filled with water during all titration experiments. The dispersion with the nanocapsules inside the sample cell was permanently stirred at 250 rpm. To determine the heat of dilution, the human serum was titrated to water. For this blank experiment, the same concentration of the human serum as in the titration experiments was used. After the measurements, the analysis of the measured curve gives the correlation between thermal flow and time. Positive peaks stand for exothermic reactions corresponding to a negative enthalpy and negative peaks stand for endothermic reactions corresponding to a positive enthalpy. Figure 1 in Supporting Information shows the typical curves created from the raw data of the titration of human serum to nanocapsules. The blank values were subtracted from values of the titration of human serum.

RESULTS AND DISCUSSION

The formation of polymeric capsules was achieved through a cross-linking reaction between the OH groups of the hydrophilic hyaluronic acid and the NCO groups of the 2,4-toluene diisocyanate (TDI), performed at the interface of miniemulsion droplets. Highly cross-linked, in water insoluble hyaluronic acid-based capsules (HA-NCs) with sulforhodamin SR101 as dye were obtained. After the synthesis, the obtained polymeric nanocapsules were transferred in water using Lutensol AT50 (0.1%) as stabilizer. For a second capsule system, polyhexanide was used as antimicrobial agent for the encapsulation into HA nanocapsules. However, because polyhexanide processes amino groups, a reaction of the polyhexanide and the TDI is even preferred compared to the reaction with OH groups leading to capsules with a mixed polymer shell (HES-PH-NCs). Polyhexanide was also used as only macromolecule for the shell formation (PH-NCs) and served as control sample since an enzymatic cleavage by hyaluronic acid is not expected. As further control capsules consisting of hydroxyethyl starch (HES) (HES-NCs) and hydroxyethyl starch/polyhexanide nanocapsules (HES-PH-NCs) were synthesized, which are expected to be resistant to the hyaluronidase. To monitor the release from the capsules, the fluorescent dye SR101 was encapsulated inside each of the nanocapsules. The formulation process is shown in Figure 2. In all cases, no precipitation, coagulation or flocculation of the capsules was observed throughout the preparation of the nanocapsules.

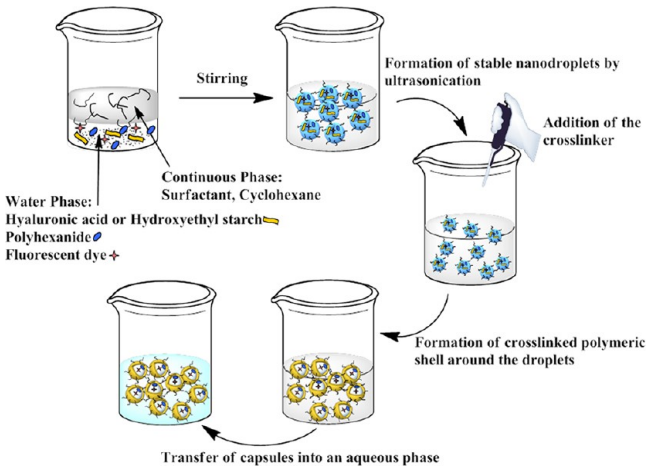

Figure 2. Schematic illustration of the nanocapsules formation through interfacial polyaddition reaction in the inverse miniemulsion system.

After the capsule's formation and their redispersion in an aqueous Lutensol AT50 solution, the size and size distribution of the nanocapsules was studied using DLS and SEM. The average size of the initial droplets/final nanocapsules in the cyclohexane phase was found to be between 210 and 360 nm depending on the used shell material. After redispersion in the aqueous phase, the DLS values slightly increased due to the formation of a Lutensol AT50 hydration layer around the capsules. The obtained DLS values for the hyaluronic acid-based nanocapsules HA-NCs and HA-PH-NCs were in the range between 360 and 380 nm with a standard deviation of about 30%. The sizes of PH-NCs, HES-NCs and HES-PH-NCs were between 230 and 260 nm (standard deviation 30%).

The morphology of the obtained nanocapsules was studied using SEM and TEM, see Figure 3. The SEM and TEM images show clearly a capsule morphology in all cases. From the images, it could be seen that the shell thickness is within 10^{-12} nm which corresponds nicely with the expected value (calculated using the amounts of reactants and the diameter of the nanocapsules). The average capsule size in the SEM and TEM images is slightly smaller than that measured by DLS, as a result of the drying. In the SEM images, the collapse of the capsules' wall is due to drying effects.

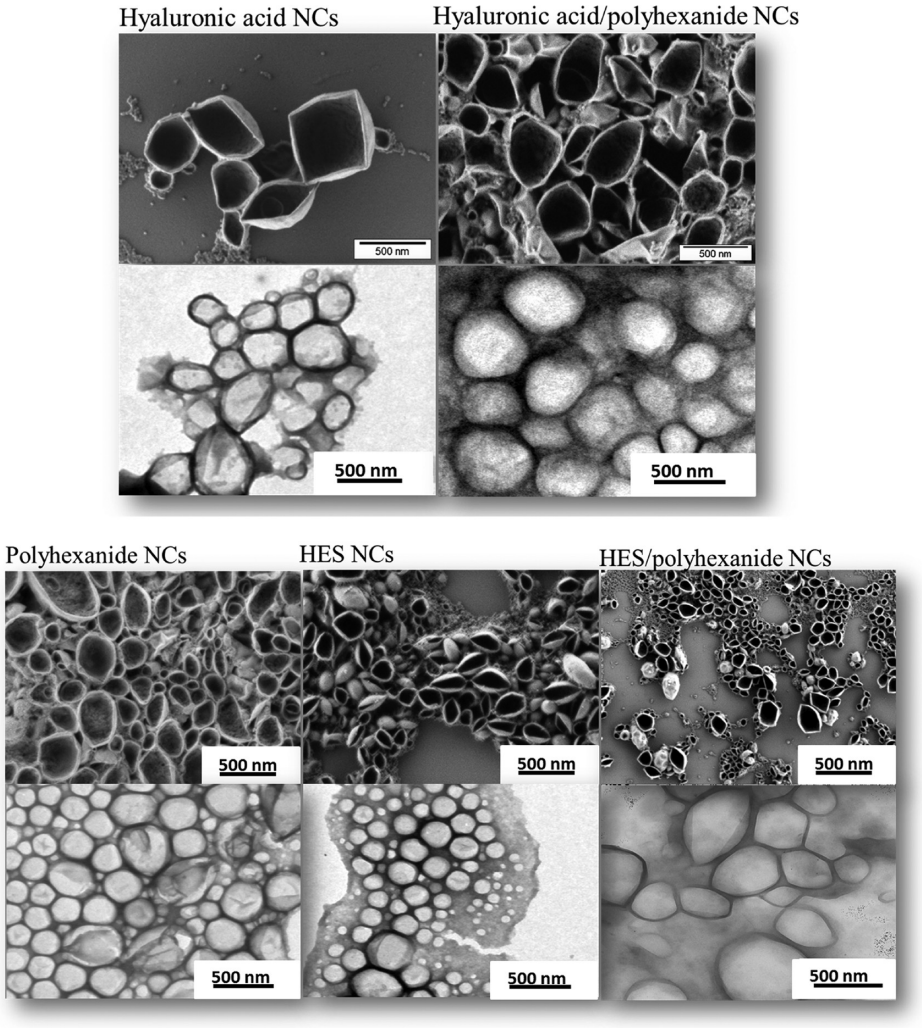

Figure 3. SEM (first row) and TEM images (second row) of cross-linked nanocapsules.

The zeta potentials (measured in 10^{-3} M potassium chloride solution, pH 6.8) of the redispersed and purified hyaluronic based and hyaluronic/polyhexanide based nanocapsules is negative (HA-NCs, −36 mV; and HA-PH- NCs, −17 mV) due to the presence of carboxylic groups on the surface of HA-based nanocapsules. For the PH-based nanocapsules, a positive zeta potential was obtained (PH-NCs, +20 mV; and HES-PH-NCs, +13 mV), which originates from the surface amine groups. For the HES nanocapsules, a slightly negative zeta potential was measured (HES-NCs, −5 mV) which is due to free hydroxyl chains from the surfactant Lutensol AT50. This could be explained by adsorption of hydroxyl ions at the nanocapsule/water interface.[30]

The chemical composition of nanocapsules was studied on dried nanocapsules from the aqueous phase by FT-IR spectroscopy. The spectra are shown in Figure 4.

All samples have strong bands characteristic for an oxygen-bonded O−H stretching vibration at 3300 cm^{-1}. The N−H valence vibration at 3250 cm^{-1} is overlapped by the O−H vibration band. However, for the three polyhexanide-containing samples, HA-PH-NCs (colored dark yellow), HES-PH-NCs (colored gray) and PH-NCs (colored black), the N−H valence can be seen at about 3200 cm^{-1}. The vibrations at 2900 cm^{-1} are from the CH_2 groups and the C−H valence vibration of the aromatic system is around 2850 cm^{-1}. The peaks between 2500 and 2000 cm^{-1} correspond to nitrogen related vibrations and include the combination of the peaks originated from nitrogen−carbon bonds in the biguanide. The peak at around 2200 cm^{-1} is assigned to N−H/C−N/C═N (combination of

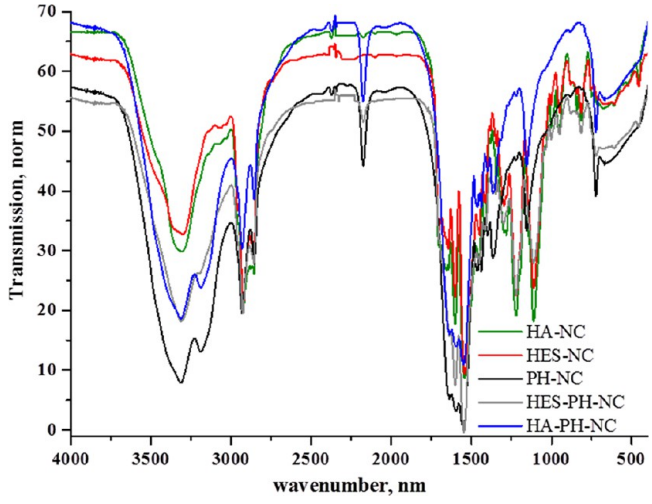

Figure 4. FT-IR spectra of the hyaluronic acid based, hyaluronic acid/polyhexanide based, polyhexanide based, hydroxyethyl starch and hydroxyethyl starch/polyhexanide cross-linked nanocapsules.

dx.doi.org/10.1021/bm302003m | *Biomacromolecules* 2013, 14, 1103−1112

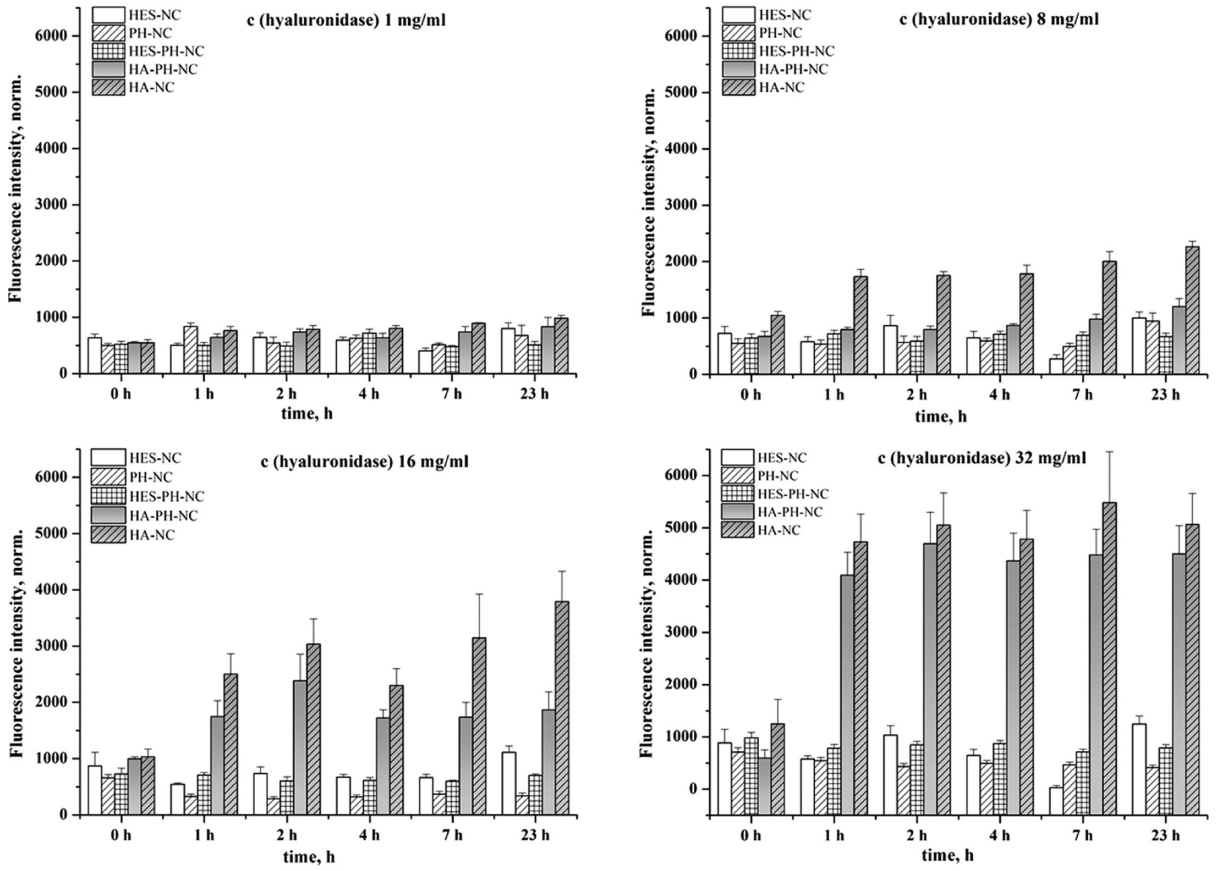

Figure 5. Release data for different nanocapsules obtained from the fluorescence spectroscopy at various time periods (0, 1, 2, 4, 7, and 23 h) using different concentrations of hyaluronidase (1, 8, 16, and 32 mg·mL^{-1}).

$-[N(H)]_2-C{=}N-$) and N−H (bound, from amide) or C−H (ν), C−C (ν), C−H (δ) and C−C (δ) originated from the pseudoaromatic biguanide ring.[19]

Encapsulation Efficiency and Release of Encapsulated Fluorescent Dye out of NCs. In a first experiment, the encapsulation efficiency of the fluorescent dye SR101 was determined from fluorescence measurements. Due to the stability of the fluorescence intensity over the broad range of pH, SR101 was chosen as a suitable model substance to study the encapsulated amount which is related to the permeability of the wall. Previously it was shown that this dye SR101 does not react with the cross-linker TDI; it does not influence the reaction mechanism and the kinetic of the polyaddition reaction, as well as the final size and morphology of the nanocapsules.[31] The yield of the encapsulated amount was in the range of 89 and 94% (HA-NCs (89%), HES-NCs (90%), PH-NCs (91%), HA-PH-NCs (94%) and HES-PH-NCs (94%)). The slightly higher values for PH-NCs and HA-PH-NCs samples could be due to the ionic interaction between positively charged PH and negatively charged SR101. The loss of SR101 could be due to the damage of the nanocapsules during the centrifugation process.

For the enzyme-triggered release from the nanocapsules, SR101 dye was used to monitor the release kinetics. The redispersed nanocapsules were treated with different concentrations of hyaluronidase (32, 16, 8, and 1 mg/mL), and after given time periods (0, 1, 2, 4, 7, and 23 h), the fluorescence intensities in the supernatant were determined (see Figure 5).

It can be seen that the increase in hyaluronidase concentrations results in higher amounts of SR101 that are released within 23 h from the nanocapsules. At all concentrations, the control samples with non-hyaluronidase sensitive polymer capsules (HES-NCs, HES-PH-NCs, PH-NCs), show a fluorescence signal of below 1000 au; this limited release can be assigned to the damage of the nanocapsules during the centrifugation process.

After incubation of the nanocapsules with the lowest concentration of hyaluronidase (1 mg·mL^{-1}), no significant difference between the amounts of the released material from different capsules was observed. At the concentration of 8 mg·mL^{-1}, mainly the nanocapsules that are composed of HA show a significant release of the dye. For the hyaluronic acid/polyhexanide nanocapsules (HA-PH-NCs), the destruction of the polymeric shell could be seen with an enzyme concentration of 16 mg·mL^{-1}. From the kinetic studies, it could be seen that within 23 h the amount of released material increases by a factor of 3 using 16 mg·mL^{-1} and by a factor of 5 when 32 mg·mL^{-1} enzyme was used.

Release of Encapsulated Polyhexanide and Cleavage of NCs. To monitor the cleavage and the release of polyhexanide from the nanocapsules with a mixed shell (HA-PH-NCs and HES-PH-NCs), two different experiments were performed: In a first experiment the released polyhexanide was measured in the supernatant using UV spectroscopy. Aqueous solutions of PHMB show no absorption in the visible range, but a strong band at 236 nm (ε = 1297 m^2·mol^{-1}) attributed to a

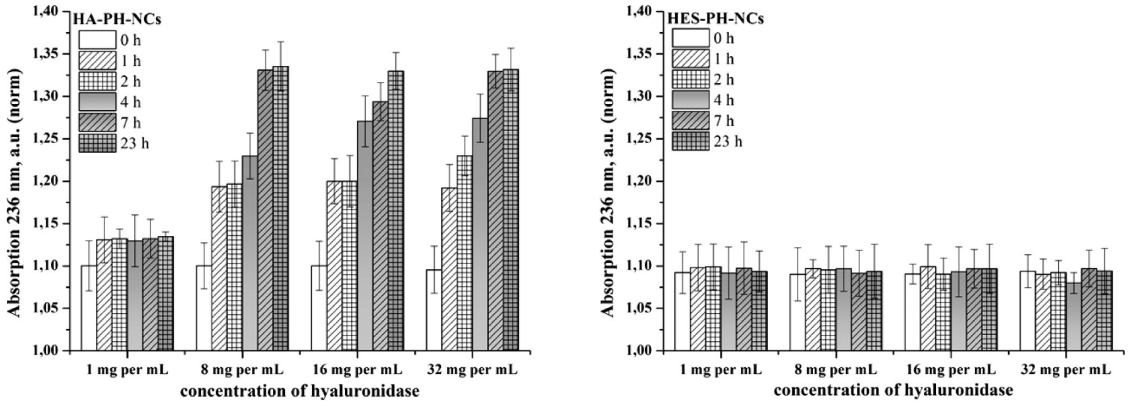

Figure 6. Release data obtained from the absorbance (236 nm) at given time periods (0, 1, 2, 4, 7, and 23 h) using different concentrations of hyaluronidase (32, 16, 8, and 1 mg/·mL^{-1}).

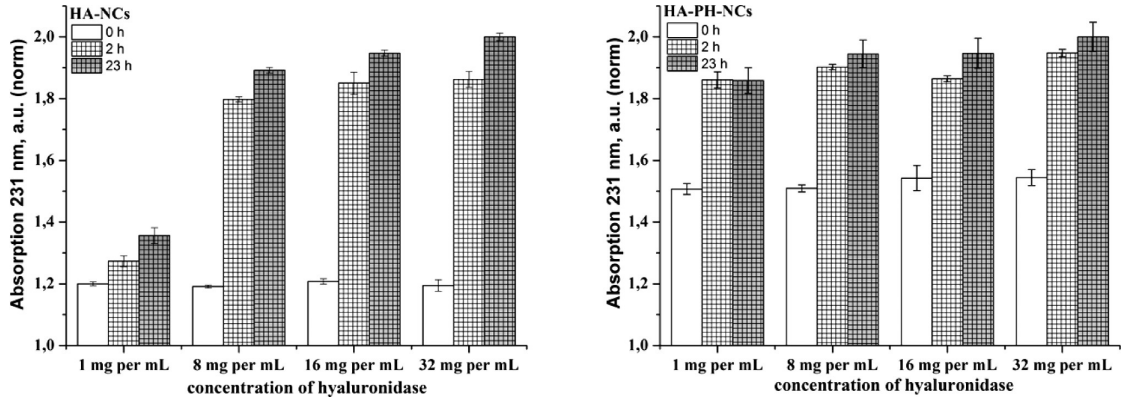

Figure 7. Cleavage data obtained from the absorbance (231 nm) at given time periods (0, 2, and 23 h) using different concentrations of hyaluronidase (1, 8, 16, and 1 mg·mL^{-1}).

$\pi-\pi^*$ transition of −C═N− in the biguanide group.[32] The experimental setup is described above (Materials and Methods); the obtained results are depicted in Figure 6.

From Figure 6, it can be seen that no polyhexanide was released from the HES-NCs independently of the used amount of hyaluronidase. For the HA-PH-NCs, a release of PH from the nanocapsules was obtained in the case of >8 mg·mL^{-1}; a concentration of 1 mg·mL^{-1} hyaluronidase was too small to trigger a significant release.

In a second experiment, the cleavage of the nanocapsules (HA-NCs and HA-PH-NCs) was studied using UV spectroscopy again. Therefore, the absorbance of the nanocapsules dispersion at 231 nm was detected; the results are depicted in Figure 7. The cleavage of hyaluronic acid to unsaturated fragments using bacterial enzymes can be monitored by measuring the absorbance at 231 nm. The enzyme catalyzed cleavage of glycosidic bonds between acetylglucosamine and glucuronic acid leads to a double bond which can be detected using UV spectroscopy.[33]

From Figure 7, it can be seen that independent of the use of PH for the shell formation, a release was observed. For the HA-PH-NCs, the cleavage of the nanocapsules can be already measured at a low concentration of 1 mg·mL^{-1}. With 8 mg·mL^{-1} or more, no difference could be observed. Using HES-NCs and HES-PH-NCs as control samples (results not shown), no cleavage at all was detected as expected.

The average size, size distribution and morphology of the five different nanocapsules before and after enzyme treatment were measured using DLS and SEM under the same conditions as described in the Materials and Methods (see above). The obtained DLS results in terms of size and size distribution are shown in Table 2 and the SEM images are depicted in Figure 8.

Table 2. Diameter and Standard Deviations (STD) Obtained from DLS Measurements before and after Enzyme Treatment

sample	diameter, nm/STD, % before enzyme treatment	diameter, nm/STD, % after enzyme treatment
HA-NCs	350, 33	500, 41 (Peak 1)
		350, 37 (Peak 2)
HA-PH-NCs	320, 33	550, 45 (Peak 1)
		400, 36 (Peak 2)
PH-NCs	260, 30	285, 34
HES-NCs	230, 28	230, 31
HES-PH-NCs	245, 28	260, 32

The size and size distribution of the hyaluronic acid based nanocapsules increased significantly (see Table 2). SEM images of the cross-linked nanocapsules, taken before and after 8 and 24 h of hyaluronidase exposure (Figure 8), show already after 8 h a clear disintegration of the nanocarrier system. After 24 h, only a few nanocapsules in terms of intact wall and morphology remained due to the presence of the hyaluronidase. In comparison, non-hyaluronic acid based nanocapsules do not change upon hyaluronidase treatment as can be seen from the size and size distribution after the hyaluronidase treatment; a

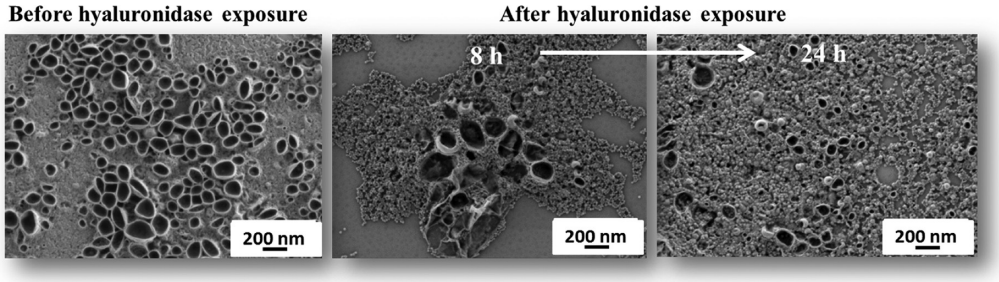

Figure 8. SEM images of cross-linked hyaluronic acid nanocapsules (HA-NCs) before and after 8 and 24 h hyaluronidase exposure.

slight increase of the size distribution might be due to the residuals from the enzyme which is attached to the nanocapsules surface. However, the size and size distribution of the hyaluronic acid based nanocapsules increased more than 8% (peak 1) and a second peak was observed. This clearly indicates the destruction of the nanocarrier system. SEM images of cross-linked nanocapsules were taken after 8 and 24 h of hyaluronidase exposure (Figure 8). Looking at these images, it can be seen that already after 8 h a destruction of the nanocapsules has taken place and the morphology vanished. After 24 h, only a few nanocapsules with intact wall and morphology have remained due to the presence of the hyaluronidase.

Antibacterial Activity of Nanocapsules *in Vitro*. Antimicrobial tests were performed against *S. aureus* ATCC 29213, *S. aureus* ATCC 43300 and *E. coli* ATCC 25922 with different concentrations of nanocapsules ranging from 1000 to 1.9 $\mu g \cdot mL^{-1}$. The minimum inhibitory concentration (MIC) study showed that the PH-NCs exhibited the same antibacterial activity as the HA-PH-NCs against both strains of *S. aureus*, preventing detectable growth at 62.5 $\mu g \cdot mL^{-1}$ *in vitro*. *E. coli* ATCC 25922 exhibited a higher resistance to the nanocapsules having a MIC of 250 and 125 $\mu g \cdot mL^{-1}$ for HA-PH-NCs and PH-NCs, respectively (see Table 3). The results show that PH-NCs inhibit bacteria growth and the combination of HA and PH showed the same activity against *S. aureus*. This can be attributed to the cleavage of the HA in the presence of *S. aureus* allowing the PH to be released from the capsules. The difference in activity between the HA-PH-NCs and PH-NCs observed against *E. coli* can be attributed to the distribution and amount of PH within the capsule walls. The HES-PH-NCs, also containing PH, showed no activity which can be attributed to the fact that the bacteria do not cleave HES.

Table 3. MIC of Nanocapsules against *S. aureus* ATCC 29213, *S. aureus* ATCC 43300 and *E. coli* ATCC 25922 ($\mu g \cdot mL^{-1}$)

	bacteria		
samples	*S. aureus* ATCC 29213	*S. aureus* ATCC 43300	*E. coli* ATCC 25922
HA-NCs	>1000	>1000	>1000
HA-PH-NCs	62.5	62.5	250.0
PH-NCs	62.5	62.5	125.0
HES-NCs	>1000	>1000	>1000
HES-PH-NCs	>1000	>1000	>1000

The ability of the HA-PH-NCs and PH-NCs to kill bacteria was defined in terms of the minimal bactericidal concentration (MBC). The MBC reveals the concentration required for complete killing of the bacteria within the well. As it can be expected, the MBC (shown in Table 4) was higher than the MIC and was 125 and 500 $\mu g \cdot mL^{-1}$ to prevent any growth of *S. aureus* and *E. coli*, respectively. These results indicate that the nanocapsules are bactericidal against both gram-positive and gram-negative bacteria. However, bacterial species which express hyaluronidase will be more susceptible to HA-PH-NCs due to HA cleavage and subsequent release of any trapped PH.

Table 4. MBC of HA-PH-NCs and PH-NCs against *S. aureus* ATCC 29213, *S. aureus* ATCC 43300, and *E. coli* ATCC 25922 ($\mu g \cdot mL^{-1}$)

	bacteria		
samples	*S. aureus* ATCC 29213	*S. aureus* ATCC 43300	*E. coli* ATCC 25922
HA-PH-NCs	125	125	500
PH-NCs	125	125	500

Stability of Nanocapsules in Different Biological Media. In the view of potential applications of the obtained nanocapsules in a wound environment, the stability of nanocapsules was analyzed in NaCl 0.9%, Ringer's solution, DBPS, human serum and CASO broth. The experiments were performed to ensure that the nanocapsules' stability is not affected by the presence of NaCl 0.9% and compounds in the Ringer's solution, DBPS, human serum or CASO broth.

Sodium chloride (NaCl) is often used in cell biology, molecular biology, and biochemistry experiments because of its isotonic character. In addition, it will not sting when applied to injured skin. Ringer's solution is isotonic compared to extracellular body fluid and is intended for intravenous administration and regularly used for the fluid resuscitation after blood or fluid loss due to trauma, surgery, or burn injuries. The experiments with DPBS were performed because this buffer is commonly used in the cellular uptake experiments and in the biological applications. Human serum was used to investigate the influence of the protein mixture on the nanoparticles' stability. CASO broth is a medium with a high concentration of nutrient and is used for growing bacteria in various microorganism tests.

The nanocapsules that were treated with the different solutions were analyzed in terms of size and size distribution by DLS. The obtained results revealed that the size and size distribution does not change upon the use of NaCl 0.9% and Ringer's solution. The same diameters and size distributions as for the nanocapsules redispersed in Lutensol AT50 solution (0.1%) were obtained. Using DPBS led to a slight increase in

diameter size (about 20 nm) and size distribution (about 5%). For the human serum and CASO broth, an increase in size of about 55 nm and in size distribution of about 7% in both cases was observed, which we assume is a result of adsorbed biomolecules from human serum and CASO broth on the surface of nanocapsules.

The release of SR 101 from the nanocapsules which is related to the stability of the nanocapsules' shell was studied by fluorescence spectroscopy. The measured fluorescence intensities of the supernatant that were obtained after precipitation of the nanocapsules treated with NaCl 0.9%, Ringer's solution, DPBS, human serum or CASO broth were compared with the nontreated ones (nanocapsules redispersed in an aqueous Lutensol AT50 solution). The calculated differences in the fluorescence intensities between treated and not treated nanocapsule samples are plotted in Figure 9.

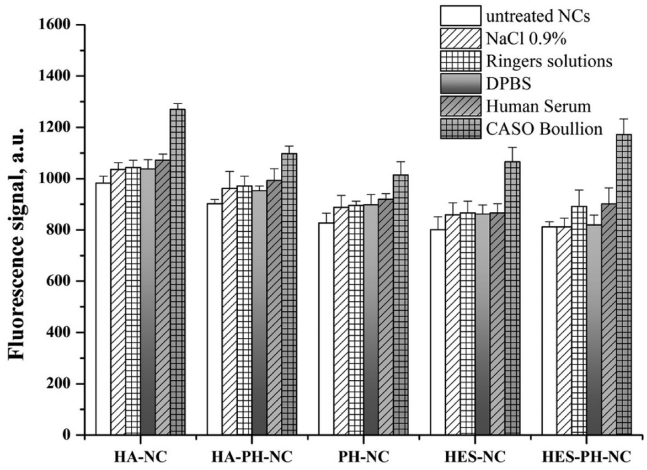

Figure 9. Amount of fluorescent dye SR101 released from the nanocapsules after incubation for 24 h at 37 °C in different biological media.

The fluorescence signal measured in the supernatant for the NaCl 0.9%, Ringer's solution, DBPS, human serum and CASO broth treated samples is almost the same as for the control samples (nontreated samples), indicating the high stability of all polymeric nanocapsules under the investigated conditions (incubation time 24 h at 37 °C).

Isothermal Titration Experiments (ITC). Whenever nanocapsules get in contact with biological media or with a wound environment, they interact immediately with the proteins. Therefore, a good knowledge about the protein layer that covers the nanocapsules is essential. One of the recently established methods to characterize the interactions between molecules regarding the thermodynamics is isothermal titration calorimetry (ITC). In this study, ITC was used to analyze the interactions of the proteins and the nanocapsules in order to get the resulting enthalpies from the adsorption of human serum to hyaluronic acid based nanocapsules (HA-NCs), hyaluronic acid/polyhexanide based nanocapsules (HA-PH-NCs), polyhexanide based nanocapsules (PH-NCs), HES based nanocapsules (HES-NCs) and HES/polyhexanide based nanocapsules (HES-PH-NCs, see Figure 1 in Supporting Information). From the plots, it can be seen that the adsorption of human serum to HES-NCs results in lower enthalpies compared with the other curves. This might be due to the "PEG"-effects because polysaccharides have proven to be a good alternative for PEG for the reduction or prevention of protein adsorption.[34] The curve obtained from the adsorption of human serum to hyaluronic acid/polyhexanide nanocapsules show the highest heat values compared with the hyaluronic acid or polyhexanide based nanocapsules. One explanation could be that the free polyhexanide chains protrude into the continuous phase. This could be seen as well in a positive zeta potential (+20 mV). Because the cationic character of the polyhexanide chains, the ionic interactions between the antimicrobial agent and the carboxylic groups from human serum proteins the ionic interactions are higher than for hyaluronic acid or polyhexanide based nanocapsules. Furthermore, the carboxylic groups from the hyaluronic acid react slower during the polyaddition reaction (with the NCO-groups originated from the diisocyanate) than the OH-groups from the hyaluronic acid. After the reaction, the COOH-groups are still present at the nanocapsules' surface and can interact with the cationic groups from the polyhexanide as well.

CONCLUSION

In the present work, the hyaluronidase triggered release of polyhexanide from hyaluronic-based nanocapsules could be shown for the first time. Stable cross-linked hyaluronic acid-based nanocapsules with trapped polyhexanide were obtained using the inverse miniemulsion technique. The nanocapsules could be cleaved by hyaluronidase; the release of the encapsulated polyhexanide was investigated by measuring the absorbance. Control capsules formed with hydroxyethyl starch or only polyhexanide as shell material did not show any release. When studied in the presence of *S. aureus* and *E. coli*, it was observed that both the polyhexanide containing, hyaluronic acid-based and the polyhexanide-based nanocapsules exhibited antibacterial action. From the minimum bactericidal concentration, it was shown that these capsules were bactericidal to *S. aureus* and *E. coli*. However, the minimum inhibitory concentration was lower for *S. aureus* due to the ability of these bacteria to cleave hyaluronic acid. The minimum inhibitory concentration was equal for both hyaluronic acid-based nanocapsules with entrapped polyhexanide and polyhexanide-based nanocapsules. The studies related to the stability of the nanocapsules in different media indicating the high stability of all polymeric nanocapsules. The adsorption of human serum to hydroxyethyl starch nanocapsules results in lower enthalpies compared with the curves obtained for the other samples. The curve obtained from the adsorption of human serum to hyaluronic acid/polyhexanide nanocapsules show the highest heat values compared with the hyaluronic acid or polyhexanide based nanocapsules. The next studies will focus on the immobilization of hyaluronic acid based nanocapsules on wound textiles with the encapsulated antimicrobial agent polyhexanide followed by their exposure to different pathogenic bacteria strains to prove their ability to prevent infections.

ASSOCIATED CONTENT

Supporting Information

Raw curves obtained from the ITC measurements. This material is available free of charge via the Internet at http://pubs.acs.org.

AUTHOR INFORMATION

Corresponding Author

*E-mail: landfester@mpip-mainz.mpg.de. Tel.: +49(0)6131 379-170. Fax: +49(0)6131 379-370.

Notes

The authors declare no competing financial interest.

■ ACKNOWLEDGMENTS

The authors thank Elke Muth for FTIR measurements, Gunnar Glasser and Christoph Sieber for his help in TEM and SEM measurements. This study was financially supported within the EU FP7 program "BacterioSafe" grant#245500.

■ REFERENCES

(1) Stern, R. *Hyaluronan in Cancer Biology*; Academic Press-Elsevier: San Diego, CA, 2009
(2) Hynes, W. *Front. Biosci.* **2004**, *9*, 3399−3433.
(3) Percival, S.; Cutting, K. *Microbiology of Wounds*; CRC Press: Boca Raton, FL, 2010.
(4) Hynes, W. L.; Walton, S. L. *FEMS Microbiol. Lett.* **2000**, *183* (2), 201−207.
(5) Hart, M. E.; Hart, J. M.; Roop, A. J. *Int. J. Microbiol.* **2009**, *2009*, No. 614371.
(6) Stern, R.; Kogan, G.; Jedrzejas, M. J.; Soltes, L. *Biotechnol. Adv.* **2007**, *25* (6), 537−557.
(7) Pirnazar, P.; Wolinsky, L.; Nachnani, S.; Haake, S.; Pilloni, A.; Bernard, G. W. *J. Periodontol.* **1999**, *70* (4), 370−374.
(8) Ardizzoni, A.; Neglia, R. G.; Baschieri, M. C.; Cermelli, C.; Caratozzolo, M.; Righi, E.; Palmieri, B.; Blasi, E. *J. Mater. Sci.: Mater. Med.* **2011**, *22* (10), 2329−2338.
(9) Alexander, S. A.; Donoff, R. B. *J. Surg. Res.* **1979**, *27* (3), 163−167.
(10) Ouasti, S.; Kingham, P. J.; Terenghi, G.; Tirelli, N. *Biomaterials* **2012**, *33* (4), 1120−1134.
(11) Vazquez, J. R.; Short, B.; Findlow, A. H.; Nixon, B. P.; Boulton, A. J. M.; Armstrong, D. G. *Diabetes Res. Clin. Pract.* **2003**, *59* (2), 123−127.
(12) Gao, F.; Yang, C. X.; Mo, W.; Liu, Y. W.; He, Y. Q. *Clin. Invest. Med.* **2008**, *31* (3), E106−E116.
(13) Campo, G. M.; Avenoso, A.; Campo, S.; D'Ascola, A.; Nastasi, G.; Calatroni, A. *Biochem. Pharmacol.* **2010**, *80* (4), 480−490.
(14) Jiang, D.; Liang, J.; Noble, P. W. *Physiol. Rev.* **2011**, *91* (1), 221−264.
(15) Koburger, T.; Huebner, N. O.; Braun, M.; Siebert, J.; Kramer, A. *J. Antimicrob. Chemother.* **2010**, *65* (8), 1712−1719.
(16) Hirsch, T.; Jacobsen, F.; Rittig, A.; Goertz, O.; Niederbichler, A.; Steinau, H. U.; Seipp, H. M.; Steinstraesser, L. *Hautarzt* **2009**, *60* (12), 984−990.
(17) Assadian, O.; Wehse, K.; Hübner, N.-O.; Koburger, T.; Bagel, S.; Jethon, F.; Kramer, A. *GMS Krankenhaushyg. Interdiszip.* **2011**, *6* (1), No. Doc06.
(18) Mueller, G.; Kramer, A. *J. Antimicrob. Chemother.* **2008**, *61* (6), 1281−1287.
(19) de Paula, G. F.; Netto, G. I.; Mattoso, L. H. C. *Polymers* **2011**, *3*, 928−941.
(20) Kramer, A.; Roth, B.; Muller, G.; Rudolph, P.; Klocker, N. *Skin Pharmacol. Phys.* **2004**, *17* (3), 141−146.
(21) Wiegand, C.; Abel, M.; Kramer, A.; Müller, G.; Ruth, P.; Hipler, U.-C. *GMS Krankenhaushyg. Interdiszip.* **2007**, *2* (2), No. Doc16 .
(22) Landfester, K. *Angew. Chem.* **2009**, *121* (25), 4556−4576.
(23) Landfester, K. M., A.; Mailänder, V. *J. Polym. Sci., Polym. Chem. Ed.* **2009**, *48* (3), 493−515.
(24) Baier, G.; Musyanovych, A.; Landfester, K.; Best, A.; Lorenz, S.; Mailaender, V. *Macromol. Biosci.* **2011**, *11* (8), 1099−1109.
(25) Schlaad, H.; Kukula, H.; Rudloff, J.; Below, I. *Macromolecules* **2001**, *34* (13), 4302−4304.
(26) Baier, G.; Musyanovych, A.; Dass, M.; Theisinger, S.; Landfester, K. *Biomacromolecules* **2010**, *11* (4), 960−968.
(27) Crespy, D.; Stark, M.; Hoffmann-Richter, C.; Ziener, U.; Landfester, K. *Macromolecules* **2007**, *40* (9), 3122−3135.
(28) Desalegu., M.; Pigman, W. *Arch. Biochem. Biophys.* **1967**, *120* (1), 60.
(29) Desalegu., M.; Plonska, H.; Pigman, W. *Arch. Biochem. Biophys.* **1967**, *121* (3), 548.
(30) Marinova, K. G.; Alargova, R. G.; Denkov, N. D.; Velev, O. D.; Petsev, D. N.; Ivanov, I. B.; Borwankar, R. P. *Langmuir* **1996**, *12* (8), 2045−2051.
(31) Vorlop, K. D.; Muscat, A.; Beyersdorf, J. *Biotechnol. Tech.* **1992**, *6* (6), 483−488.
(32) Nandi, S. D. *Tetrahedron* **1972**, *28* (3), 845−&.
(33) Jandik, K. A.; Gu, K. A.; Linhardt, R. J. *Glycobiology* **1994**, *4* (3), 289−296.
(34) Besheer, A.; Vogel, J.; Glanz, D.; Kressler, J.; Groth, T.; Mader, K. *Mol. Pharmaceutics* **2009**, *6* (2), 407−415.